

## OBSERVATION OF THE TEV GAMMA-RAY SOURCE MGRO J1908+06 WITH ARGO-YBJ

B. BARTOLI<sup>1,2</sup>, P. BERNARDINI<sup>3,4</sup>, X.J. BI<sup>5</sup>, C. BLEVE<sup>3,4</sup>, I. BOLOGNINO<sup>6,7</sup>, P. BRANCHINI<sup>8</sup>, A. BUDANO<sup>8</sup>, A.K. CALABRESE MELCARNE<sup>9</sup>, P. CAMARRI<sup>10,11</sup>, Z. CAO<sup>5</sup>, R. CARDARELLI<sup>11</sup>, S. CATALANOTTI<sup>1,2</sup>, C. CATTANEO<sup>7</sup>, S.Z. CHEN<sup>5</sup>, T.L. CHEN<sup>15</sup>, Y. CHEN<sup>5</sup>, P. CRET<sup>4</sup>, S.W. CUI<sup>16</sup>, B.Z. DAI<sup>17</sup>, G. D'ALÌ STAITI<sup>18,19</sup>, DANZENGLUOBU<sup>15</sup>, M. DATTOLI<sup>12,13,20</sup>, I. DE MITRI<sup>3,4</sup>, B. D'ETTORRE PIAZZOLI<sup>1,2</sup>, T. DI GIROLAMO<sup>1,2</sup>, X.H. DING<sup>15</sup>, G. DI SCIASCIO<sup>11</sup>, C.F. FENG<sup>21</sup>, ZHAOYANG FENG<sup>5</sup>, ZHENYONG FENG<sup>22</sup>, F. GALEAZZI<sup>8</sup>, E. GIROLETTI<sup>6,7</sup>, Q.B. GOU<sup>5</sup>, Y.Q. GUO<sup>5</sup>, H.H. HE<sup>5</sup>, HAIBING HU<sup>15</sup>, HONGBO HU<sup>5</sup>, Q. HUANG<sup>22</sup>, M. IACOVACCI<sup>1,2</sup>, R. IUPPA<sup>10,11</sup>, I. JAMES<sup>8,14</sup>, H.Y. JIA<sup>22</sup>, LABACIREN<sup>15</sup>, H.J. LI<sup>15</sup>, J.Y. LI<sup>21</sup>, X.X. LI<sup>5</sup>, G. LIGUORI<sup>6,7</sup>, C. LIU<sup>5</sup>, C.Q. LIU<sup>17</sup>, J. LIU<sup>17</sup>, M.Y. LIU<sup>15</sup>, H. LU<sup>5</sup>, X.H. MA<sup>5</sup>, G. MANCARELLA<sup>3,4</sup>, S.M. MARI<sup>8,14</sup>, G. MARSELLA<sup>4,23</sup>, D. MARTELLO<sup>3,4</sup>, S. MASTROIANNI<sup>2</sup>, P. MONTINI<sup>8,14</sup>, C.C. NING<sup>15</sup>, A. PAGLIARO<sup>19,24</sup>, M. PANAREO<sup>4,23</sup>, B. PANICO<sup>10,11</sup>, L. PERRONE<sup>4,23</sup>, P. PISTILLI<sup>8,14</sup>, X.B. QU<sup>21</sup>, F. RUGGIERI<sup>8</sup>, P. SALVINI<sup>7</sup>, R. SANTONICO<sup>10,11</sup>, P.R. SHEN<sup>5</sup>, X.D. SHENG<sup>5</sup>, F. SHI<sup>5</sup>, C. STANESCU<sup>8</sup>, A. SURDO<sup>4</sup>, Y.H. TAN<sup>5</sup>, P. VALLANIA<sup>12,13</sup>, S. VERNETTO<sup>12,13</sup>, C. VIGORITO<sup>13,20</sup>, B. WANG<sup>5</sup>, H. WANG<sup>5</sup>, C.Y. WU<sup>5</sup>, H.R. WU<sup>5</sup>, B. XU<sup>22</sup>, L. XUE<sup>21</sup>, Y.X. YAN<sup>17</sup>, Q.Y. YANG<sup>17</sup>, X.C. YANG<sup>17</sup>, Z.G. YAO<sup>5</sup>, A.F. YUAN<sup>15</sup>, M. ZHA<sup>5</sup>, H.M. ZHANG<sup>5</sup>, JILONG ZHANG<sup>5</sup>, JIANLI ZHANG<sup>5</sup>, L. ZHANG<sup>17</sup>, P. ZHANG<sup>17</sup>, X.Y. ZHANG<sup>21</sup>, Y. ZHANG<sup>5</sup>, ZHAXICIREN<sup>15</sup>, ZHAXISANGZHU<sup>15</sup>, X.X. ZHOU<sup>22</sup>, F.R. ZHU<sup>22</sup>, Q.Q. ZHU<sup>5</sup> AND G. ZIZZI<sup>9</sup>  
(THE ARGO-YBJ COLLABORATION)

<sup>1</sup> Dipartimento di Fisica dell'Università di Napoli "Federico II", Complesso Universitario di Monte Sant'Angelo, via Cinthia, 80126 Napoli, Italy.

<sup>2</sup> Istituto Nazionale di Fisica Nucleare, Sezione di Napoli, Complesso Universitario di Monte Sant'Angelo, via Cinthia, 80126 Napoli, Italy.

<sup>3</sup> Dipartimento di Fisica dell'Università del Salento, via per Arnesano, 73100 Lecce, Italy.

<sup>4</sup> Istituto Nazionale di Fisica Nucleare, Sezione di Lecce, via per Arnesano, 73100 Lecce, Italy.

<sup>5</sup> Key Laboratory of Particle Astrophysics, Institute of High Energy Physics, Chinese Academy of Sciences, P.O. Box 918, 100049 Beijing, P.R. China.

<sup>6</sup> Dipartimento di Fisica Nucleare e Teorica dell'Università di Pavia, via Bassi 6, 27100 Pavia, Italy.

<sup>7</sup> Istituto Nazionale di Fisica Nucleare, Sezione di Pavia, via Bassi 6, 27100 Pavia, Italy.

<sup>8</sup> Istituto Nazionale di Fisica Nucleare, Sezione di Roma Tre, via della Vasca Navale 84, 00146 Roma, Italy.

<sup>9</sup> Istituto Nazionale di Fisica Nucleare - CNAF, Viale Berti-Pichat 6/2, 40127 Bologna, Italy.

<sup>10</sup> Dipartimento di Fisica dell'Università di Roma "Tor Vergata", via della Ricerca Scientifica 1, 00133 Roma, Italy.

<sup>11</sup> Istituto Nazionale di Fisica Nucleare, Sezione di Roma Tor Vergata, via della Ricerca Scientifica 1, 00133 Roma, Italy.

<sup>12</sup> Osservatorio Astrofisico di Torino dell'Istituto Nazionale di Astrofisica, corso Fiume 4, 10133 Torino, Italy.

<sup>13</sup> Istituto Nazionale di Fisica Nucleare, Sezione di Torino, via P. Giuria 1, 10125 Torino, Italy.

<sup>14</sup> Dipartimento di Fisica dell'Università "Roma Tre", via della Vasca Navale 84, 00146 Roma, Italy.

<sup>15</sup> Tibet University, 850000 Lhasa, Xizang, P.R. China.

<sup>16</sup> Hebei Normal University, Shijiazhuang 050016, Hebei, P.R. China.

<sup>17</sup> Yunnan University, 2 North Cuihu Rd., 650091 Kunming, Yunnan, P.R. China.

<sup>18</sup> Università degli Studi di Palermo, Dipartimento di Fisica e Tecnologie Relative, Viale delle Scienze, Edificio 18, 90128 Palermo, Italy.

<sup>19</sup> Istituto Nazionale di Fisica Nucleare, Sezione di Catania, Viale A. Doria 6, 95125 Catania, Italy.

<sup>20</sup> Dipartimento di Fisica dell'Università di Torino, via P. Giuria 1, 10125 Torino, Italy.

<sup>21</sup> Shandong University, 250100 Jinan, Shandong, P.R. China.

<sup>22</sup> Southwest Jiaotong University, 610031 Chengdu, Sichuan, P.R. China.

<sup>23</sup> Dipartimento di Ingegneria dell'Innovazione, Università del Salento, 73100 Lecce, Italy. and

<sup>24</sup> Istituto di Astrofisica Spaziale e Fisica Cosmica dell'Istituto Nazionale di Astrofisica, via La Malfa 153, 90146 Palermo, Italy.

*ApJ*, in press

### ABSTRACT

The extended gamma ray source MGRO J1908+06, discovered by the Milagro air shower detector in 2007, has been observed for  $\sim 4$  years by the ARGO-YBJ experiment at TeV energies, with a statistical significance of 6.2 standard deviations. The peak of the signal is found at a position consistent with the pulsar PSR J1907+0602. Parametrizing the source shape with a two-dimensional Gauss function we estimate an extension  $\sigma_{ext} = 0.49^\circ \pm 0.22^\circ$ , consistent with a previous measurement by the Cherenkov Array H.E.S.S.. The observed energy spectrum is  $dN/dE = 6.1 \pm 1.4 \times 10^{-13} (E/4 \text{ TeV})^{-2.54 \pm 0.36}$  photons  $\text{cm}^{-2} \text{s}^{-1} \text{TeV}^{-1}$ , in the energy range  $\sim 1$ -20 TeV. The measured gamma ray flux is consistent with the results of the Milagro detector, but is  $\sim 2$ -3 times larger than the flux previously derived by H.E.S.S. at energies of a few TeV. The continuity of the Milagro and ARGO-YBJ observations and the stable excess rate observed by ARGO-YBJ along 4 years of data taking support the identification of MGRO J1908+06 as the steady powerful TeV pulsar wind nebula of PSR J1907+0602, with an integrated luminosity above 1 TeV  $\sim 1.8$  times the Crab Nebula luminosity.

*Subject headings:* gamma rays: general - pulsars: individual (MGRO J1908+06)

### 1. INTRODUCTION

The Galactic gamma ray source MGRO J1908+06 was discovered by the Milagro air shower detector in a survey of the Galactic plane at a median energy of  $\sim 20$  TeV (1). The data

were consistent both with a point source and with an extended source of diameter  $< 2.6^\circ$ . Assuming a spectrum  $\propto E^{-2.3}$ , the measured flux at the median energy of 20 TeV is  $8.8 \pm 2.4 \times 10^{-15}$  photons  $\text{cm}^{-2} \text{s}^{-1} \text{TeV}^{-1}$ .

A marginal detection of a source consistent with the position of MGRO J1908+06 was already reported by the Tibet

AS- $\gamma$  array (33), but not confirmed in a more recent paper (16).

The source was later observed by the H.E.S.S. (9) and VERITAS (32) Cherenkov telescopes. In particular, H.E.S.S. detected an extended source (HESS J1908+063) at energies above 300 GeV ( $\sim 11$  standard deviations of statistical significance) positionally consistent with MGRO J1908+06. The measured source extension, evaluated assuming a symmetrical two-dimensional Gaussian shape, was  $\sigma_{ext} = 0.34^{+0.04}_{-0.03}$ .

H.E.S.S. reported a power law differential energy spectrum with a photon index of  $2.10 \pm 0.07_{stat} \pm 0.2_{sys}$  in the energy range 0.3-20 TeV, and a flux at 1 TeV of  $(4.14 \pm 0.32_{stat} \pm 0.83_{sys}) \times 10^{-12}$  photons  $\text{cm}^{-2} \text{s}^{-1} \text{TeV}^{-1}$ . The integrated flux above 1 TeV is 17% that of the Crab Nebula.

After the release of the Bright Source List by the Fermi collaboration (3), Milagro reported the association of MGRO J1908+06 to the LAT pulsar 0FGL J1907.5+0602 (later named PSR J1907+0602), pulsating with a period of 106.6 ms (4). The peak of the Milagro emission was  $0.3^\circ$  off the pulsar, but consistent with the pulsar location within the measurement error ( $0.27^\circ$ ). Assuming a spectrum  $\propto E^{-2.6}$ , Milagro reported a flux of  $116.7 \pm 15.8 \times 10^{-17}$  photons  $\text{cm}^{-2} \text{s}^{-1} \text{TeV}^{-1}$ , at the median energy of 35 TeV.

The association of MGRO J1908+06 with PSR J1907+0602 was also supported in (5), where a multiwavelength study of the pulsar and the surrounding region has been performed with radio, X-ray and Fermi gamma ray data. Because of the small angular distance between the pulsar and the centroid of the H.E.S.S. extended source, the authors argue that the latter is plausibly the Wind Nebula of the pulsar.

Performing an off-pulse measurement, Fermi set an upper limit to the HESS J1908+063 flux in the energy region 0.1-25 GeV, suggesting that the spectrum has a low-energy turnover between 20 GeV and 300 GeV. With radio and X-ray data, a lower limit to the pulsar distance was set to  $\sim 3.2$  kpc, deriving for the nebula a physical size  $\geq 40$  pc.

Later, Milagro evaluated the energy spectrum of the source in the 2-100 TeV region, reporting a hard power law spectrum with an exponential cutoff (Smith 2009). The best fit obtained is  $dN/dE = 0.62 \times 10^{-11} E^{-1.50} \exp(-E/14.1)$  photons  $\text{cm}^{-2} \text{s}^{-1} \text{TeV}^{-1}$ , where E is the energy in TeV. This flux is in disagreement with that given by H.E.S.S. at a level of 2-3 standard deviations, being about a factor 3 higher at 10 TeV. The authors suggest that the discrepancy can be simply due to a statistical fluctuation, or to the fact that Milagro, given its relatively poor angular resolution, integrates the signal over a larger solid angle compared with H.E.S.S., and likely detects more of the diffuse lateral tails of the extended source.

In this work we report on the observation of MGRO J1908+06 with the ARGO-YBJ detector performed during the years 2007-2011. After a brief description of the detector and a detailed presentation of the data analysis technique, we report our results concerning the extension and the energy spectrum of the source.

## 2. THE ARGO-YBJ EXPERIMENT

The ARGO-YBJ detector is located at the Yangbajing Cosmic Ray Laboratory (Tibet, China) at an altitude of 4300 m above sea level. It consists of a  $\sim 74 \times 78 \text{ m}^2$  carpet made of a single layer of Resistive Plate Chambers (RPCs) with  $\sim 92\%$  of active area, surrounded by a partially instrumented ( $\sim 20\%$ ) area up to  $\sim 100 \times 110 \text{ m}^2$ . The apparatus has a modular structure, the basic data acquisition element being a cluster

( $5.7 \times 7.6 \text{ m}^2$ ), made of 12 RPCs ( $2.8 \times 1.25 \text{ m}^2$ ). The RPCs are operated in streamer mode by using a gas mixture (Ar 15%, Isobutane 10%, TetraFluoroEthane 75%) suitable for high altitude operation.

Each RPC is read by 80 strips of  $6.75 \times 61.8 \text{ cm}^2$  (the spatial pixels), logically organized in 10 independent pads of  $55.6 \times 61.8 \text{ cm}^2$  which are individually acquired and represent the time pixels of the detector (10). In addition, in order to extend the dynamical range up to PeV energies, each RPC is equipped with two large size pads ( $139 \times 123 \text{ cm}^2$ ) to collect the total charge developed by the particle hitting the detector (25). The full experiment is made of 153 clusters for a total active surface of  $\sim 6600 \text{ m}^2$ .

ARGO-YBJ operates in two independent acquisition modes: the *shower mode* and the *scaler mode* (11). In this analysis we refer to the data recorded from the digital readout in shower mode. In this mode, an electronic logic has been implemented to build an inclusive trigger, based on a time correlation between the pad signals, depending on their relative distances. In this way, all the shower events giving a number of fired pads  $N_{pad} \geq N_{trig}$  in the central carpet in a time window of 420 ns generate the trigger. This trigger can work with high efficiency down to  $N_{trig}=20$ , keeping negligible the rate of random coincidences (15).

The time of each fired pad in a window of  $2 \mu\text{sec}$  around the trigger time and its location are recorded and used to reconstruct the position of the shower core and the arrival direction of the primary particle.

In order to perform the time calibration of the 18360 pads, a software procedure has been developed, based on the Characteristic Plane method (24) which using the secondary particles of large vertical showers as calibration beams, iteratively reduces the differences between the measured times and the temporal fit of the shower front (12).

The full detector is in stable data taking since 2007 November with the trigger condition  $N_{trig}=20$  and a duty cycle  $\sim 86\%$ . The trigger rate is  $\sim 3.5 \text{ kHz}$  with a dead time of 4%.

## 3. DETECTOR PERFORMANCE

The angular resolution and the pointing accuracy of the detector have been evaluated by using the Moon shadow, i.e. the deficit of cosmic rays in the Moon direction, observed by ARGO-YBJ with a statistical significance of  $\sim 9$  standard deviations per month. The shape of the shadow provides a measurement of the detector Point Spread Function (PSF), and its position allows the individuation of possible pointing biases.

The data have been compared with the results of a Monte Carlo simulation which describes the propagation of cosmic rays in the Earth magnetic fields, the shower development in the atmosphere by using the CORSIKA code (23), and the detector response with a code based on the GEANT package (22). The PSF measured with the cosmic rays has been found in excellent agreement with the Monte Carlo evaluation, confirming the reliability of the simulation procedure (18).

The angular resolution for gamma rays is evaluated by simulating the events from a gamma ray source with a given spectrum and daily path in the sky. It results smaller by  $\sim 30\text{-}40\%$  compared with the angular resolution for cosmic rays, due to the better defined time profile of the showers. In general, the PSF for gamma rays can be described by the sum of two Gaussian distributions. For a Crab-like source, the radius of the opening angle which optimizes the signal-to-background ratio for events with  $N_{pad} \geq 60$  (300) is  $0.86^\circ$  ( $0.44^\circ$ ) and con-

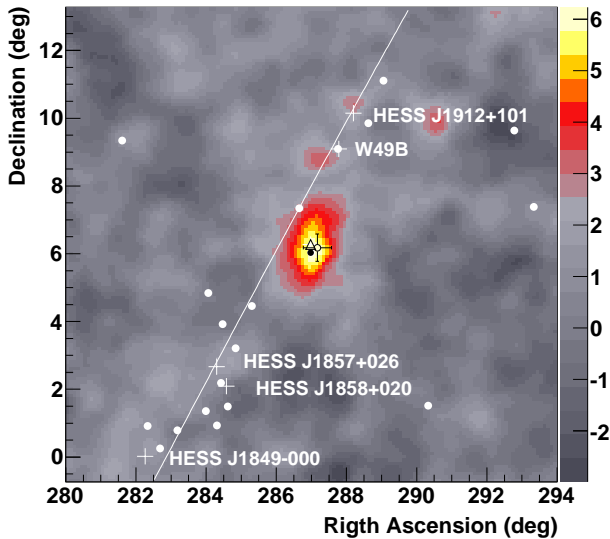


FIG. 1.— PSF-smoothed significance map of the MGRO J1908+06 region obtained by ARGO-YBJ, for events with  $N_{pad} \geq 60$ . Open circle: position of the center of MGRO J1908+06, as measured by Milagro. The error bars give the linear sum of the statistical and systematic errors. Open triangle: centroid of HESS J1908+063. Black filled circle: Fermi pulsar PSR J1907+0602. White filled circles: Fermi gamma ray sources, according to the 2nd Fermi Catalogue (27). White crosses: TeV sources detected by H.E.S.S. in the same region. The white line represents the Galactic plane.

tains  $\sim 50\%$  of the signal.

The Moon Shadow has also been used to check the absolute energy calibration of the detector, by studying the westward shift of the shadow due to the geomagnetic field. The observed displacement as a function of the event multiplicity  $N_{pad}$  is in excellent agreement with the results of the Monte Carlo simulation. From this analysis the total absolute energy scale error, including systematic effects, is estimated to be less than 13% (18).

#### 4. DATA ANALYSIS AND RESULTS

At the ARGO-YBJ site MGRO J1908+06 culminates at the zenith angle of  $24^\circ$  and is visible for 5.38 hours per day with a zenith angle less than  $45^\circ$ . The dataset used in this analysis refers to the period from November 2007 to December 2011 and contains all the showers with zenith angle less than  $45^\circ$  and  $N_{pad} \geq 20$ . The total on-source time is 6867 hours.

To study the gamma ray emission from a source, a  $16^\circ \times 16^\circ$  sky map in celestial coordinates (right ascension and declination) with  $0.1^\circ \times 0.1^\circ$  bin size, centered on the source position, is filled with the detected events.

In order to extract the excess of gamma rays, the cosmic ray background has to be estimated and subtracted.

The *time swapping* method (14) is used to evaluate the background: for each detected event,  $n$  "fake" events (with  $n = 10$ ) are generated by replacing the original arrival time with new ones, randomly selected from an event buffer which spans a time  $T$  of data taking. Changing the time, the fake events maintain the same declination of the original event, but have a different right ascension. With these events a new sky map (background map) is built, with a statistics  $n$  times larger than the "true" event map in order to reduce the fluctuations. To avoid the inclusion of the source events in the background

evaluation, the showers inside a circular region around the source (with a radius related to the PSF and depending on  $N_{pad}$ ) are excluded from the time swapping procedure. A correction of the number of swaps is made to take into account the rejected events in the source region (21). The value of the swapping time  $T$  is  $\sim 3$  hours, in order to minimize the systematic effects due to the environmental parameter variations.

In order to extract the source signal the maps are smoothed according to the detector PSF, determined by Monte Carlo simulations for different  $N_{pad}$  intervals. Finally, the smoothed background map is subtracted to the smoothed event map, obtaining the "excess map", where for every bin the statistical significance  $S$  of the excess is given by:

$$S = (N_{on} - N_{off}) / \sqrt{\delta N_{on}^2 + \delta N_{off}^2}$$

with  $N_{on} = \sum_i N_i w_i$  and  $N_{off} = \sum_i B_i w_i / n$ . In these expressions  $N_i$  and  $B_i$  are the number of events of the  $i^{th}$  bin of the "event map" and "background map", respectively,  $w_i$  is a weight proportional to the value of the PSF at the angular distance of the  $i^{th}$  bin, and  $n$  is the number of swaps. The sum is over all the bins inside a radius  $R$ , chosen to contain the PSF. Since the number of events per bin is large, the fluctuations follow the Gaussian statistics, hence the errors on  $N_{on}$  and  $N_{off}$  are:  $\delta N_{on} = \sqrt{\sum_i N_i w_i^2}$  and  $\delta N_{off} = \sqrt{\sum_i B_i w_i^2 / n^2}$ .

In order to study the signal in different energy regions, the maps are built for 8 different  $N_{pad}$  intervals, namely 20-39, 40-59, 60-99, 100-199, 200-299, 300-499, 500-999, and  $>1000$ . These maps are then combined to have "integral maps" for different  $N_{pad}$  thresholds.

Analysing the data recorded in 4 years, the sky maps of the MGRO J1908+06 region show a significant excess at the source position for different  $N_{pad}$  thresholds. The larger significance is given by events with  $N_{pad} \geq 20$ , with 7.3 standard deviations. Increasing  $N_{pad}$ , the significance decreases. For  $N_{pad} > 1000$  no signal is present.

The distributions of the significances outside the source region follow a standard normal distribution, showing the correctness of the background evaluation procedure.

As will be discussed in Section 4.3, the signal with  $N_{pad}=20-59$  is largely affected by the Galactic diffuse gamma ray flux, and only events with  $N_{pad} \geq 60$  will be used in the study of the source morphology and flux. Fig.1 shows the significance map for events with  $N_{pad} \geq 60$ , where the source signal reaches 6.2 standard deviations.

Studying the source on the time scale of one year, the annual excess rate results to be consistent with the total average rate, indicating that the gamma ray flux from MGRO J1908+06 is likely due to a steady emission.

##### 4.1. Source position and extension

To evaluate the position and extension of the source, the events with  $N_{pad} \geq 60$  are used. We assume a source shape described by a symmetrical two-dimensional Gaussian function with r.m.s.  $\sigma_{ext}$ . Fitting the non-smoothed excess map to a function given by the convolution of the above Gaussian and the detector PSF, we found the best-fit position at R.A. =  $19^h 08^m 1^s$  and decl. =  $6^\circ 24'$ , with a statistical error of  $12'$  and a systematic error of  $6'$  per axis. The position found is consistent with the the Milagro measurement and with the centroid of HESS J1908+063 (R.A. =  $19^h 07^m 54^s$  and decl. =  $6^\circ 16' 7''$ , with a statistical error of  $2.4'$  and a systematic error of  $20''$  per axis).

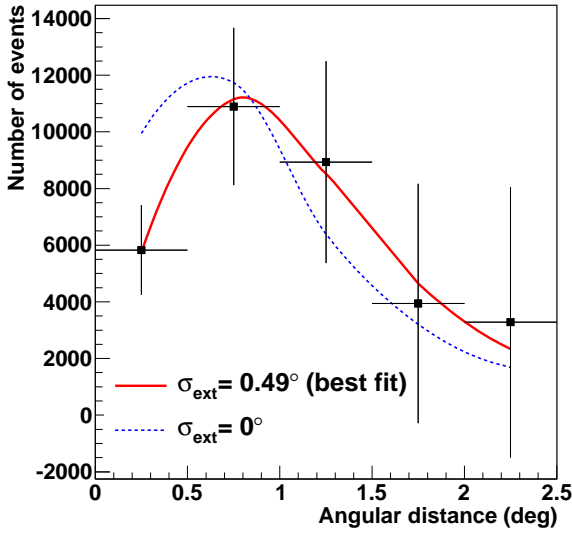


FIG. 2.— Number of excess events with  $N_{pad} \geq 60$  as a function of the angular distance from the best-fit centroid position, compared with the expected distributions for different source extensions.

The value of  $\sigma_{ext}$  that best fits the data is  $0.49^\circ \pm 0.22^\circ$ , consistent with the H.E.S.S. estimation of  $0.34^\circ$ .

Fig.2 shows the distribution of the angular distance from the best-fit centroid position, compared with the simulated distributions corresponding to the extensions  $\sigma_{ext}=0.49^\circ$  and  $\sigma_{ext}=0^\circ$ . The two curves are normalized to the same number of excess events.

#### 4.2. Energy spectrum

In order to study the energy dependence of the signal the events are divided in different subsets according to the number of hit pads, and a sky map is built for each subset. For this analysis we define 4 intervals:  $N_{pad} = 20-59$ ,  $60-199$ ,  $200-499$  and  $N_{pad} \geq 500$ . The intervals have been chosen in order to have a signal of comparable statistical significance.

For the spectrum evaluation we assume a power law dependence:  $dN/dE = K E^{-\gamma}$ . The values of  $K$  and  $\gamma$  are derived by comparing the number of the excess events detected in each of the previously defined  $N_{pad}$  intervals with the corresponding ones given by simulations assuming a set of test spectra. The reliability of this procedure has been tested studying the Crab Nebula signal (13).

For each  $N_{pad}$  interval, the number of excess events is obtained integrating the sky map around the source position up to a distance  $\psi_{max}$ , where  $\psi_{max}$  is the radius of the opening angle which maximizes the signal to background ratio. The value of  $\psi_{max}$  depends on the source extension  $\sigma_{ext}$  and on the detector PSF, and is provided by simulations. For the extension we use the value  $\sigma_{ext} = 0.49^\circ$ , according to our measurement. On the other hand, the PSF for a given  $N_{pad}$  interval is not precisely determined, since it depends both on the detector characteristics and on the spectrum index  $\gamma$ , which is unknown. To solve this ‘‘circular’’ problem an iterative procedure has been applied.

First, an initial index  $\gamma = 2.5$  is assumed, and the corresponding values of  $\psi_{max}$  for every  $N_{pad}$  interval are determined via simulations. The number of events observed in  $\psi_{max}$  are then used to evaluate a new spectral slope  $\gamma$  which

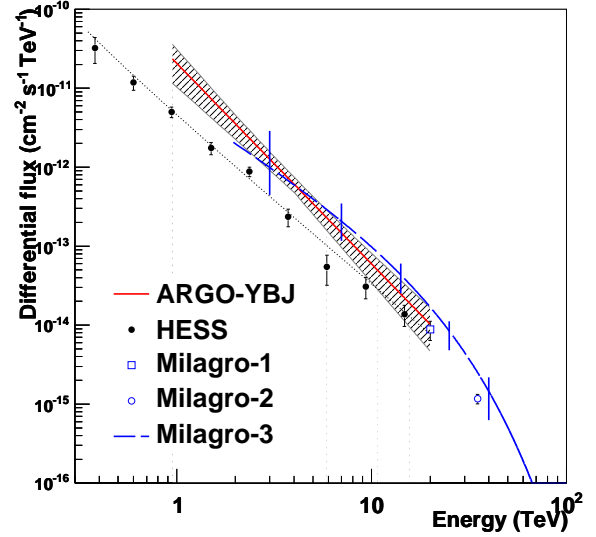


FIG. 3.— Gamma ray flux from MGRO J1908+06 measured by different detectors. ARGO-YBJ: the continuous line (colored red in the online version) is the best fit to data. The dashed area represents the one standard deviation error. H.E.S.S.: the dotted line is the best fit to the points (9). Milagro 1: flux value assuming a spectrum  $\propto E^{-2.3}$  (1). Milagro 2: flux value assuming a spectrum  $\propto E^{-2.6}$  (4). Milagro 3: the dashed line (colored blue in the online version) is the spectrum fit according to Smith (2009) and the vertical lines are the errors (at one standard deviation) for some values of the energy. The plotted errors are purely statistical for all the detectors.

is returned to the first step, to calculate a new set of  $\psi_{max}$ , and so on. Given the relatively weak dependence of the PSF on  $\gamma$ , a small number of iterations is sufficient to terminate the process successfully and provide the parameters of the best fit spectrum.

#### 4.3. Contribution from diffuse flux

Since the source is located on the Galactic plane, the observed flux could be affected by the diffuse gamma ray emission produced by cosmic rays interacting with the matter and the radiation fields of the Galaxy. Given the relatively large opening angles used in the measurement, the photons from the diffuse radiation falling in the observational window of MGRO J1908+06 could artificially increase the flux detected from the source direction. The amount of this contribution can be evaluated by analysing the data collected from the Galactic plane region close to the source.

The flux of very high energy Galactic gamma rays in the region of MGRO J1908+06 (Galactic coordinates  $l = 40.39^\circ$  and  $b = -0.79^\circ$ ) is poorly known.

The first evidence of a diffuse Galactic emission at TeV energies has been reported by the Milagro detector (17). A significant dependence of the flux on the Galactic latitude and longitude has been found in a later analysis with events of median energy 15 TeV (2). The same paper reports the expected energy spectrum for two different sectors of the Galactic plane, for energies from 10 keV to 100 TeV, according to the GALPROP model (29; 28), ‘‘optimized’’ to fit the measurements by EGRET in the 40 MeV - 10 GeV energy range and by Milagro at 15 TeV. Concerning the MGRO J1908+06 region, the expected average flux at 1 TeV in the area of Galactic coordinates  $l \in [30^\circ, 65^\circ]$  and  $b \in [-2^\circ, 2^\circ]$  is

$\sim 2 \times 10^{-9}$  photons  $\text{TeV}^{-1} \text{cm}^{-2} \text{s}^{-1} \text{sr}^{-1}$ .

A preliminary flux measurement at energies  $E > 300$  GeV, obtained with the ARGO-YBJ data, is reported by Ma (2011), who derives the average gamma ray spectrum for  $l \in [25^\circ, 65^\circ]$  and  $b \in [-2^\circ, 2^\circ]$ . This estimate results lower but still consistent with the expectation of the above model.

For our purposes, given the variation of the emission along the Galactic plane and its strong dependence on the latitude, it is preferable to evaluate the diffuse flux in a restricted region, adjacent to the source position.

We consider two sky regions,  $L_1$  and  $L_2$ , of size  $\Delta l = 5^\circ$  and  $\Delta b = 2 \times \psi_{max}$  (where  $\psi_{max}$  depends on the  $N_{pad}$  interval) whose centers have the same latitude of MGRO J1908+06 and are located at both sides of the source, at a longitudinal distance of  $5.5^\circ$ .

Analysing the ARGO-YBJ data, a global excess of statistical significance 3.0 standard deviations over the cosmic ray background is observed in  $L_1 + L_2$  for events with  $N_{pad} > 20$ . This excess is interpreted as due to the diffuse Galactic emission plus the contribution of 5 gamma ray sources discovered by H.E.S.S., namely HESS J1912+101 (8), W49B (20), HESS J1857+026 and HESS J1858+020 (7), and HESS J1849-000 (30).

The individual fluxes of these objects are below the ARGO-YBJ sensitivity, while the total flux is  $(29 \pm 3)\%$  that of the Crab Nebula at 1 TeV (31). In particular, HESS J1912+101 and HESS J1857+026 have a flux  $\sim 10\%$  and  $\sim 17\%$  that of the Crab Nebula, respectively. The number of events from these sources expected to fall in  $L_1$  and  $L_2$  is evaluated via simulations, using the fluxes measured by H.E.S.S., and gives a global contribution of  $(40 \pm 14)\%$  to the observed diffuse excess. After the subtraction of this contribution, taking into account the different exposures of  $L_1$  and  $L_2$ , we evaluate the number of events due to the diffuse emission expected to fall into the observational window of MGRO J1908+06.

We found that the ratio between the number of events expected from the diffuse emission and those observed from the source direction is  $R_d = 0.33 \pm 0.18$  for showers with  $N_{pad} = 20-59$ , and  $R_d < 0.15$  (at one sigma level) for showers with  $N_{pad} \geq 60$ .

As a comparison, the values derived by using the ‘‘optimized’’ GALPROP diffuse emission model given by Abdo et al. (2008) are  $R_d = 0.57$  for  $N_{pad} = 20-59$ , and  $R_d = 0.23$  for  $N_{pad} \geq 60$ . These values are larger than those obtained with the ARGO-YBJ data. It should be noted, however, that the above model is based on a measurement by Milagro which does not take into account all the gamma ray sources located in the studied region, and could overestimate the diffuse flux.

The larger contribution of the diffuse emission for  $N_{pad} = 20-59$  is due to the wider opening angle used in this interval ( $\psi_{max} = 2.0^\circ$ ). Because of these estimates, to avoid a possible large systematic effect in the flux evaluation, we restrict our spectral analysis to the events with  $N_{pad} \geq 60$ .

Performing the procedure described in Section 4.2, we fit the data of the 3 intervals  $N_{pad} = 60-199$ ,  $200-499$  and  $N_{pad} \geq 500$ . The best fit spectrum obtained is:  $dN/dE = 6.1 \pm 1.4 \times 10^{-13} (E/4 \text{ TeV})^{-2.54 \pm 0.36}$  photons  $\text{cm}^{-2} \text{s}^{-1} \text{TeV}^{-1}$ , valid in the energy region 1-20 TeV. The median energies corresponding to the 3  $N_{pad}$  intervals are 2.4, 5.1 and 12.8 TeV, respectively.

As a comparison, if we do not exclude the data with  $N_{pad} = 20-59$ , the best-fit spectrum is:  $dN/dE = 1.36 \pm 0.29 \times 10^{-12} (E/3 \text{ TeV})^{-2.65 \pm 0.25}$  photons  $\text{cm}^{-2} \text{s}^{-1} \text{TeV}^{-1}$ , which

gives a flux 21% higher at  $E = 1$  TeV.

Beside the statistical errors and the systematics due to the diffuse contribution discussed before, our measurement could be affected by an additional systematic error mainly due to the background evaluation, to the absolute energy scale determination, to the pointing accuracy, to environmental effects and to the Monte Carlo simulations, for a global effect that we estimate to be  $< 30\%$  (Aielli et al. 2010).

In the case of an extended source, a possible further cause of systematics could be the uncertainty in the extension, and the consequent use of an incorrect opening angle to extract the signal. Therefore we have also evaluated the spectrum assuming  $\sigma_{ext} = 0.34^\circ$ , as measured by H.E.S.S. The resulting flux differs from the previous one by less than 5% in the whole energy range considered in the analysis.

The obtained spectrum is shown in Fig.3, together with those reported by H.E.S.S. and Milagro. The flux is significantly higher than that given by H.E.S.S. in the 1-10 TeV energy range, but is consistent with the Milagro spectrum (Smith 2009). The hard spectrum with exponential cutoff obtained by Milagro produces a worse, but still acceptable, fit to our data. Given the reduced significance of the excess at high energies, we are not able to constrain the shape of the spectrum above 10 TeV and to definitively rule out a high energy cutoff.

## 5. DISCUSSION AND CONCLUSIONS

The gamma ray source MGRO J1908+06 has been studied by ARGO-YBJ analyzing  $\sim 4$  years of data. An excess with significance 6.2 standard deviations is observed in a position consistent with previous measurements by Milagro and H.E.S.S.. The peak of the signal occurs at R.A. =  $19^h 08^m 1^s$  and decl. =  $6^\circ 24'$  (with statistical and systematic errors of  $\sim 0.2^\circ$  and  $0.1^\circ$  per axis, respectively) and lies at a distance of  $22'$  from PSR J1907+0602, consistent with the pulsar location within the measurement error.

The signal is due to emission from an extended region. After taking into account the detector PSF, the extension of the source is found to be  $\sigma_{ext} = 0.49^\circ \pm 0.22^\circ$ .

The photon spectrum in the range 1-20 TeV follows a simple power law with a spectral index  $2.54 \pm 0.36$ , though a harder spectrum with a high energy cutoff cannot be ruled out.

The spectrum is found to be consistent with the Milagro result (Smith 2009) but not with the H.E.S.S. best fit in the 1-10 energy range, the flux measured by ARGO-YBJ at 4 TeV being a factor 2.6 larger. At  $\sim 20$  TeV the ARGO-YBJ, H.E.S.S. and Milagro fluxes are consistent within the errors, and are also in agreement with the first Milagro measurement (1).

Since a contribution to this measurement is expected from the Galactic diffuse emission, data from two sky regions located at both sides of the source and centered at the same latitude have been used to determine this contamination. According to this estimate, the diffuse Galactic gamma ray emission is expected to contribute to the signal above 1 TeV for less than  $\sim 15\%$ , and cannot account for the observed disagreement.

Being the difference with H.E.S.S. at the level of 2.5 standard deviations, the discrepancy could be simply due to statistical fluctuations, or to the combination of statistical and systematic uncertainties. However these latter have been accurately studied, giving a global error on the flux less than 30%. Indeed, the spectrum of the Crab Nebula obtained by ARGO-YBJ results to be in good agreement with the Cherenkov de-

tectors measurements (13; 31). The extension of the source should not give such an additional systematic error to explain the observed difference.

On the other hand, a similar discrepancy is found in the observation of the extended source MGRO J2031+41, located in the Cygnus region, for which ARGO-YBJ (19) and Milagro (6) report a flux significantly larger than that measured by the Cherenkov Telescopes MAGIC and HEGRA.

In principle, one cannot exclude the possibility of a flux variation as the origin of the observed disagreement among the detectors. Milagro, H.E.S.S. and ARGO-YBJ data have been recorded in different periods. Milagro integrates over seven years (July 2000 - November 2007) while the total H.E.S.S. data set only amounts to 27 hours of sparse observations during 2005-2007, before the ARGO-YBJ measurement. However, a possible flux variation seems unlikely, since the average fluxes measured by Milagro and ARGO-YBJ in two contiguous periods covering a total time of 11 years, are consistent.

Moreover, it should be noted that if MGRO J1908+06 is the pulsar wind nebula associated to PSR J1907+0602, the gamma ray emission originates from a region whose size has been estimated to be  $\geq 40$  pc (5), implying that the variation

time scale cannot be less than  $\sim 130$  years, unless relativistic beaming effects are present.

In conclusion, MGRO J1908+06 is observed by ARGO-YBJ as a stable extended source, likely the TeV nebula of PSR J1907+0602, with a flux at 1 TeV  $\sim 67\%$  that of the Crab Nebula. Assuming a distance of 3.2 kpc, the integrated luminosity above 1 TeV is  $\sim 1.8$  times that of the Crab Nebula, making MGRO J1908+06 one of the most luminous Galactic gamma ray sources at TeV energies.

This work is supported in China by NSFC (No. 10120130794), the Chinese Ministry of Science and Technology, the Chinese Academy of Science, the Key Laboratory of Particle Astrophysics, CAS, and in Italy by the Istituto Nazionale di Fisica Nucleare (INFN).

We also acknowledge the essential support of W.Y. Chen, G. Yang, X.F. Yuan, C.Y. Zhao, R. Assiro, B. Biondo, S. Bricola, F. Budano, A. Corvaglia, B. D'Aquino, R. Esposito, A. Innocente, A. Mangano, E. Pastori, C. Pinto, E. Reali, F. Taurino, and A. Zerbini, in the installation, debugging, and maintenance of the detector.

#### REFERENCES

- Abdo, A.A., Allen, B., Berley, D., et al. 2007, *ApJ*, 664, L91  
 Abdo, A.A., Allen, B., Aune, T., et al. 2008, *ApJL* 688, 1078  
 Abdo, A.A., Ackermann, M., Ajello, M., et al. 2009a, *ApJS* 183, 46  
 Abdo, A.A., Allen, B.T., Aune, T., et al. 2009b, *ApJ*, 700, L27  
 Abdo, A.A., Ackermann, M., Ajello, M., et al. 2010, *ApJ* 711, 64  
 Abdo, A.A., Abeysekara, U., Allen, B.T., et al. 2012, *ApJ*, 753, 159  
 Aharonian, F., Akhperjanian, A.G., Barres de Almeida, U., et al. 2008a, *A&A*, 477, 353  
 Aharonian, F., Akhperjanian, A.G., Barres de Almeida, U., et al. 2008b, *A&A*, 484, 435  
 Aharonian, F., Akhperjanian, A.G., Anton, G., et al. 2009, *A&A*, 499, 723  
 Aielli, G., Assiro, R., Bacci, C., et al. 2006, *Nucl. Instrum. Methods Phys. Res. A*, 562, 92  
 Aielli, G., Bacci, C., Barone, F., et al. 2008, *Astrop. Phys.*, 30, 85  
 Aielli, G., Bacci, C., Bartoli, B., et al. 2009, *Astrop. Phys.*, 30, 287  
 Aielli, G., Bacci, C., Bartoli, B., et al. 2010, *ApJ*, 714, L208  
 Alexandreas, D.E., Berley, D., Biller, S., et al. 1993, *Nucl. Instrum. Methods Phys. Res. A*, 328, 570  
 Aloisio, A., Branchini, P., Catalanotti, S. et al. 2004, *IEEE Transaction on Nuclear Science*, 51, 1835  
 Amenomori, M., Bi, X.J., Chen, D., et al. 2010, *ApJ*, 709, L6  
 Atkins, R., Benbow, W., Berley, D., et al. 2005, *Phys. Rev. Lett.* 95, 251103  
 Bartoli, B., Bernardini, P., Bi, X.J., et al. 2011, *Phys. Rev. D*, 84, 022003  
 Bartoli, B., Bernardini, P., Bi, X.J., et al. 2012, *ApJ*, 745, L22  
 Brun, F., De Naurois, M., Hofmann, W., et al. 2011, in Proc. 25th Texas Symposium on Relativistic Astrophysics (available at arXiv:1104.5003v1)  
 Fleysher, R., Fleysher, L., Nemethy, P., & Mincer, A.I. 2004, *ApJ*, 603, 355  
 GEANT - Detector Description and Simulation Tool 1993, CERN Program Library, W5013, <http://www.wasd.web.cern.ch/www.wasd/geant/>  
 Heck, D., Knapp, J., Capdevielle, J.N., Shatz, G., & Thouw, T. 1998, Forschungszentrum Karlsruhe Report No. FZKA 6019  
 He, H.H., Bernardini, P., Calabrese Melcarne, A.K., Chen, S.Z. 2007, *Astropart. Physics*, 27, 528  
 Iacovacci, M., Corvaglia, A., Creti, P., et al. 2009, in Proc. 31st Int. Cosmic Ray Conf., Lodz, Poland (available at <http://icrc2009.uni.lodz.pl/proc/html/>)  
 Ma, L.L. 2011, in Proc. 32nd Int. Cosmic Ray Conf., Beijing, China (available at <http://www.ihep.ac.cn/english/conference/icrc2011/paper/>)  
 Nolan, P.L., Abdo, A.A., Ackermann, M., et al. 2011, *ApJS*, in press (arXiv: 1108.1435)  
 Porter, T.A., Moskalenko, I.V., Strong, A.W., Orlando, E., & Bouchet, L. 2008, *ApJ* 682, 400  
 Smith, A.J. 2009, in Proc. Fermi Symposium, Conf Proceedings C091122, <http://www.slac.stanford.edu/econf/C0911022/>  
 Strong, A.W., Moskalenko, I.V., Reimer, O. 2000, *ApJ*, 537, 763  
 Terrier, R., Mattana, F., Djannati-Atai, A., et al 2008, in Proc. 4th Int. Meeting on High Energy Gamma-Ray Astronomy, AIP Conference Proceedings, 1085, 312  
 Vernetto, S. 2011, in Proc. 32nd Int. Cosmic Ray Conf., Beijing, China (available at <http://www.ihep.ac.cn/english/conference/icrc2011/paper/>)  
 Ward, J.E. 2008, in AIP Conf. Proc. 1085, High energy Gamma-Ray Astronomy, ed. F.A.Aharonian, W.Hofmann, & F.Rieger (Melville, NY:AIP), 301  
 Zhang, J.L. 2003, in Proc. 28th Int. Cosmic Ray Conf., Vol.4, ed. T.Kajita et al. (Tokyo: Universal Academy Press, Inc.), 2405